International Journal of Pharmaceutics 422 (2012) 398–408

Contents lists available at SciVerse ScienceDirect

International Journal of Pharmaceutics

journal homepage: www.elsevier.com/locate/ijpharm

Pharmaceutical nanotechnology

Nebulization performance of biodegradable sildenafil-loaded nanoparticles using the Aeroneb® Pro: Formulation aspects and nanoparticle stability to nebulization

Moritz Beck-Broichsitter[a,b,*], Pia Kleimann[a], Tobias Gessler[a], Werner Seeger[a], Thomas Kissel[b], Thomas Schmehl[a]

[a] Medical Clinic II, Department of Internal Medicine, Justus-Liebig-Universität Giessen, Klinikstrasse 36, D-35392 Giessen, Germany
[b] Department of Pharmaceutics and Biopharmacy, Philipps-Universität, Ketzerbach 63, D-35037 Marburg, Germany

ARTICLE INFO

Article history:
Received 23 June 2011
Received in revised form
28 September 2011
Accepted 1 October 2011
Available online 6 October 2011

Keywords:
Sildenafil
Biodegradable polyesters
Nanoparticles
Pulmonary drug delivery
Nebulization
Pulmonary arterial hypertension

ABSTRACT

Polymeric nanoparticles meet the increasing interest for drug delivery applications and hold great promise to improve controlled drug delivery to the lung. Here, we present a series of investigations that were carried out to understand the impact of formulation variables on the nebulization performance of novel biodegradable sildenafil-loaded nanoparticles designed for targeted aerosol therapy of life-threatening pulmonary arterial hypertension.

Narrowly distributed poly(D,L-lactide-*co*-glycolide) nanoparticles (size: ~200 nm) were prepared by a solvent evaporation technique using poly(vinyl alcohol) (PVA) as stabilizer. The aerodynamic and output characteristics using the Aeroneb® Pro nebulizer correlated well with the dynamic viscosity of the employed fluids for nebulization. The nebulization performance was mainly affected by the amount of employed stabilizer, rather than by the applied nanoparticle concentration. Nanoparticles revealed physical stability against forces generated during aerosolization, what is attributed to the adsorbed PVA layer around the nanoparticles. Sildenafil was successfully encapsulated into nanoparticles (encapsulation efficiency: ~80%). Size, size distribution and sildenafil content of nanoparticles were not affected by nebulization and the *in vitro* drug release profile demonstrated a sustained sildenafil release over ~120 min.

The current study suggests that the prepared sildenafil-loaded nanoparticles are a promising pharmaceutical for the therapy of pulmonary arterial hypertension.

1. Introduction

Pulmonary arterial hypertension is a severe, life threatening disease that dramatically limits exercise capacity. The increase in pulmonary artery pressure and vascular resistance with subsequent dysfunction of the right heart results in a seriously reduced life expectancy with a median survival of only 2.8 years without treatment (D'Alonzo et al., 1991). The specific drug therapy of pulmonary arterial hypertension mainly comprises the intravenous and oral application of potent vasodilators (Galie et al., 2009). One substance, sildenafil (Viagra®), belongs to the family of phosphodiesterase inhibitors and is administered orally to patients three times daily. The oral administration of sildenafil, however, results in systemic availability of the drug leading to significant side effects (Galie et al., 2005; Ghofrani et al., 2006; Wilkins et al., 2008). Meanwhile, a more selective route of administration, namely drug delivery to the lung by inhalation, has been recommended, due to its ability to circumvent unwanted systemic side effects. The direct application of a drug to the lungs facilitates a targeted treatment of respiratory diseases, as demonstrated for the prostacyclin analogue iloprost (Ventavis®) in the treatment of pulmonary arterial hypertension (Olschewski et al., 2002). However, the relatively short duration of pharmacological effects after pulmonary drug deposition is regarded as a major drawback of inhalation therapy, therefore requiring frequent drug administrations via inhalation (Gessler et al., 2008; Ichinose et al., 2001).

In this context, colloidal carriers such as polymeric nanoparticles, seem to be promising pulmonary drug delivery systems. With the direct delivery of nanoencapsulated therapeutics to the lung, sustained and controlled drug release at the desired site of action can be achieved, leading to prolonged pharmacological effects (Azarmi et al., 2008; Beck-Broichsitter et al., 2011a). The choice

* Corresponding author at: Medical Clinic II, Department of Internal Medicine, Justus-Liebig-Universität Giessen, Klinikstrasse 36, D-35392 Giessen, Germany. Tel.: +49 641 985 42453; fax: +49 641 985 42359.
E-mail address: moritz.beck-broichsitter@innere.med.uni-giessen.de (M. Beck-Broichsitter).

0378-5173/$ – see front matter © 2011 Elsevier B.V. All rights reserved.
doi:10.1016/j.ijpharm.2011.10.012

of the nanoparticle preparation technique essentially depends on the physicochemical properties of the polymeric nanoparticle matrix material intended to be used and the active compound to be encapsulated in the nanoparticles. Regarding the polymeric nanoparticle matrix material, criteria such as biocompatibility and biodegradability determine its selection (Vauthier and Bouchemal, 2009). In addition, nanoparticles need to meet further standards such as sufficient association of the therapeutic agent with the carrier and stability against forces generated during aerosolization. Nanoparticulate drug delivery systems composed of biodegradable polymers have shown to fulfill these stringent requirements (Beck-Broichsitter et al., 2009, 2010a; Lebhardt et al., 2010; Rytting et al., 2008, 2010).

The solvent evaporation technique is known to be a convenient nanoparticle preparation method. This technique comprises the emulsification of an organic polymer solution in an aqueous phase containing excipients for stabilization purpose. The employed stabilizers were often found to modulate the physicochemical and biological properties of the nanoparticle formulations (Vauthier and Bouchemal, 2009). Despite its relevance for inhalation therapy, the impact of formulation parameters on aerodynamic characteristics of nebulized formulations and on nanoparticle stability to nebulization has been so far rather underestimated for actively vibrating-mesh nebulizers (Dailey et al., 2003a; Ghazanfari et al., 2007; Zhang et al., 2007).

Therefore, the present study addressed the principles associated with nanoparticle production by the solvent evaporation technique, like polymer concentration in the organic phase and concentration of stabilizer in the aqueous phase. Furthermore, their effects on the nebulization performance employing the actively vibrating-mesh nebulizer Aeroneb® Pro were evaluated. Aerosols were characterized by laser diffraction and aerodynamic parameters were correlated with the physicochemical properties (dynamic viscosity and surface tension). Furthermore, the stability of the nanoparticles to the nebulization process was assessed by analysis of particle size, polydispersity index, ζ-potential and particle morphology. Based on these investigations, novel biodegradable sildenafil-loaded poly(D,L-lactide-*co*-glycolide) nanoparticles were designed and thoroughly characterized regarding their physicochemical characteristics before and after aerosolization. In particular, controlled release properties of the freshly prepared and nebulized sildenafil-loaded nanoparticles were determined by monitoring the *in vitro* drug release profile employing UV/Vis spectroscopy.

2. Materials and methods

2.1. Materials

Poly(D,L-lactide-*co*-glycolide) (PLGA), Resomer® RG502H, was acquired from Boehringer Ingelheim (Ingelheim, Germany). Poly(vinyl alcohol) (PVA), Mowiol® 4-88, was purchased from Sigma–Aldrich (Steinheim, Germany). Sildenafil (free base) was obtained from AK Scientific (Mountain View, USA). All other chemicals and solvents used in this study were of the highest analytical grade commercially available. The actively vibrating-mesh nebulizer Aeroneb® Pro was acquired from Aerogen (Dangan, Galway, Ireland).

2.2. Methods

2.2.1. Physicochemical characterization of fluids prepared for nebulization

2.2.1.1. Density measurements. The densities of fluids prepared for nebulization were measured using an oscillating density meter (DMA 4100 M, Anton Paar, Graz, Austria) at 25 °C. The density of each solution was calculated from the average of three repeated measurements.

2.2.1.2. Viscosity measurements. The determination of viscosities of fluids prepared for nebulization were performed at 25 °C using a temperature controlled capillary viscosimeter of the Ubbelohde type (Schott, Mainz, Germany). The viscosity of each solution was calculated from the average of five repeated measurements.

2.2.1.3. Surface tension measurements. The surface tensions of fluids prepared for nebulization were measured at 25 °C using a temperature controlled tensiometer equipped with a Wilhelmy plate (K11-Mk3, Kruess, Hamburg, Germany). The surface tension of each solution was calculated from the average of five repeated measurements.

2.2.2. Preparation of nanoparticles

Nanoparticles were synthesized using a solvent evaporation technique (Beck-Broichsitter et al., 2011b; Scholes et al., 1993; Vauthier and Bouchemal, 2009). At first, PLGA (with or without drug) was dissolved in methylene chloride. Then, 2 ml of the organic phase (dispersed phase) were transferred to 10 ml of an aqueous phase (continuous phase) containing PVA as surface active stabilizer. After initial pre-mixing of the two phases using an Ultra-Turrax® (IKA®-Labortechnik, Staufen, Germany), the emulsion was sonicated (Sonifier 250, Branson, Danbury, USA). The organic phase was then removed slowly using a rotary evaporator (Rotavapor®, Büchi, Flawil, Switzerland). Particles were characterized and used directly after preparation.

2.2.3. Characterization of nanoparticles

2.2.3.1. Size and ζ-potential measurement. The hydrodynamic diameter and size distribution of nanoparticles were measured by dynamic light scattering (DLS), and their ζ-potential was determined by laser Doppler anemometry (LDA) using a Zetasizer NanoZS/ZEN3600 (Malvern Instruments, Herrenberg, Germany). All measurements were performed at a temperature of 25 °C using samples appropriately diluted with filtrated and double distilled water for DLS and with 1.56 mM NaCl for LDA, respectively. All measurements were carried out in triplicate directly after nanoparticle preparation with at least 10 runs.

2.2.3.2. Determination of the adsorbed PVA layer thickness on nanoparticles. The thickness of the adsorbed PVA layer on nanoparticles was determined using DLS and ζ-potential measurements as a function of electrolyte concentration (Besheer et al., 2009; Shimada et al., 1995). Concerning DLS measurements, the adsorbed PVA layer thickness (δ) was derived from the comparison of the particle sizes of bare (d_0) and coated nanoparticles (d_{ads}), according to the following equation

$$\delta = \frac{d_{ads} - d_0}{2} \quad (1)$$

Layer thickness from ζ-potential measurements was calculated using the Gouy–Chapman approximation, which expresses the decrease of the electrostatic potential as a function of the distance from the surface as follows

$$\psi_x = \psi_0 \cdot e^{-\kappa x} \quad (2)$$

where ψ_x is the potential at a distance x from the surface, ψ_0 is the surface potential, and κ^{-1} is the Debye length. An increase of electrolyte concentration (NaCl) decreases the Debye length. ζ-Potentials are defined as the electrostatic potentials at the position

of the slipping plane, which is thought to occur just outside the fixed aqueous layer of a nanoparticle. From Eq. (2) follows

$$\ln\psi_x = \ln\psi_0 - \kappa \cdot x \quad (3)$$

If ζ-potentials (ψ_x) are measured in various concentrations of NaCl (0, 0.1, 0.2, 0.5, 1, 2 and 5 mM) and plotted against κ equal to $3.33c^{1/2}$, where c is the molality of electrolytes, the slope equals the thickness of the adsorbed polymer layer.

2.2.3.3. Scanning electron microscopy (SEM). A droplet of dilute nanoparticle suspension was deposited on a silica wafer. Before imaging, all samples were dried in vacuum and subsequently coated with a platinum layer using a Gatan Alto 2500 sputter coater (Gatan, München, Germany) for 90 s. The morphology of nanoparticles was observed at 2 kV using a scanning electron microscope (JSM-7500F, JEOL, Eching, Germany).

2.2.3.4. Transmission electron microscopy. The samples were prepared by coating a carbon-coated copper grid (S160-3, Plano, Wetzlar, Germany) with a thin layer of dilute nanoparticle suspension. Dried nanoparticles were then investigated using a transmission electron microscope (JEM-3010 TEM, JEOL, Eching, Germany) at an acceleration voltage of 300 kV.

2.2.3.5. Determination of entrapped sildenafil. To determine the drug content samples of nanoparticle suspensions (1 ml) were subjected to centrifugation (Centrifuge 5418, Eppendorf, Hamburg, Germany) at 16,873 × *g* for 30 min at 25 °C. After centrifugation the supernatant was carefully removed and sampled to determine the amount of unencapsulated sildenafil. The remaining pellets were freeze-dried (Beta I, Christ, Osterode, Germany), weighed, and then dissolved in chloroform (a common solvent for PLGA and sildenafil). The undissolved fraction (PVA) was removed by centrifugation. After centrifugation, a sample was taken from the organic phase to determine the amount of encapsulated sildenafil. Sildenafil concentrations were quantified by UV/Vis spectroscopy as described below. The drug content of sildenafil in the nanoparticles is defined in the following formula

$$\text{sildenafil content (\%(w/w))} = \frac{\text{mass of sildenafil in PLGA nanoparticles}}{\text{mass of PLGA nanoparticles recovered}} \times 100 \quad (4)$$

2.2.4. In vitro drug release studies

The *in vitro* drug release studies were carried out in phosphate buffered saline at a pH of 7.4 supplemented with 0.1% (w/w) sodium dodecyl sulfate (Sigma–Aldrich, Steinheim, Germany) over a 480 min period of time. The studies were performed with nanoparticles containing 5% (w/w) theoretical sildenafil loading. Samples of the nanoparticle suspensions were transferred to glass vials and diluted with the release medium (total volume: 10 ml). Incubation occurred at 37 °C with shaking. Samples were taken at preset time points and centrifuged prior to determining the cumulative release of sildenafil by UV/Vis spectroscopy. In parallel, sildenafil was incubated in the release medium under the same conditions.

2.2.5. Aerosol output

The aerosol output was determined gravimetrically by weighing the nebulizer (Aeroneb® Pro) before and after each nebulization experiment. The resulting difference in weight was used to calculate the output rate in g/min.

2.2.6. Aerosol particle size determination by laser diffraction

For aerosolization the actively vibrating-mesh nebulizer Aeroneb® Pro was employed. In order to compare the particle size distribution of the aerosolized formulations and NaCl 0.9% (*m*/*v*) as control, the volume median diameter (VMD) of the aerosol droplets was determined using laser diffraction (HELOS, Sympatec, Clausthal-Zellerfeld, Germany). The measurements were performed as previously described (Clark, 1995). All data were analyzed in Mie mode. The density of the nebulized solutions was set to unit density and thus the measured VMD equaled the mass median aerodynamic diameter (MMAD). The geometric standard deviation (GSD) was calculated from the laser diffraction values according to the following equation

$$\text{GSD} = \sqrt{\frac{d_{84\%}}{d_{16\%}}} \quad (5)$$

where d_n is the diameter at the percentile n of the cumulative distribution. The fine particle fraction (FPF) is given as the volume fraction of the aerosol with particles sizes below 5.25 μm.

2.2.7. Nanoparticle stability during nebulization

To study the stability of nanoparticles during nebulization, nebulized nanoparticle suspensions were collected and investigated as previously described (Dailey et al., 2003a,b). Briefly, samples of nanosuspensions were aerosolized at an airflow rate of 5 l/min and collected by placing a glass microscopic slide in front of the nebulizer T-shaped mouthpiece allowing the aerosol droplets to deposit on the glass. The resulting condensation fluid was collected for further analysis. The stability of the nebulized nanoparticles was investigated using DLS and SEM. In addition, the amount of encapsulated sildenafil of the aerosolized drug-loaded nanoparticles was estimated.

2.2.8. Sildenafil quantification by UV/Vis spectroscopy

Sildenafil concentrations were determined by UV/Vis spectroscopy using a spectrophotometer (Ultrospec® 3000, Pharmacia Biotech, Freiburg, Germany). Absorption of all samples was assayed at a wavelength of 291 nm. The sildenafil content was calculated using a calibration curve.

2.2.9. Statistics

All measurements were carried out in triplicate and values are presented as the mean ± S.D. unless otherwise noted. Statistical calculations were carried out using the software SigmaStat 3.5 (STATCON, Witzenhausen, Germany). To identify statistically significant differences, one-way ANOVA with Bonferroni's post *t*-test analysis was performed. Probability values of $p < 0.05$ were considered significant.

3. Results

3.1. Factors affecting the preparation of nanoparticles by the solvent evaporation technique

Nanoparticles composed of poly(D,L-lactide-*co*-glycolide) were prepared by a solvent evaporation technique. The sizes of nanoparticles are displayed as a function of the inverse of the PVA concentration ($1/c_{PVA}$) in Fig. 1A. The concentration of PLGA in the organic phase was kept constant at 50 g/l, whereas PVA concentration varied between 1 and 50 g/l. Fig. 1A clearly illustrates the linear dependency of particle size from $1/c_{PVA}$ ($R^2 = 0.991$). As the stabilizer concentration was increased, the mean particle size of obtained nanoparticles decreased to ~200 nm. PVA concentrations above 10 g/l led only to a negligible change of mean particle size of obtained nanoparticles, but to an unwanted foaming during nanoparticle preparation that caused a loss of nanoparticle

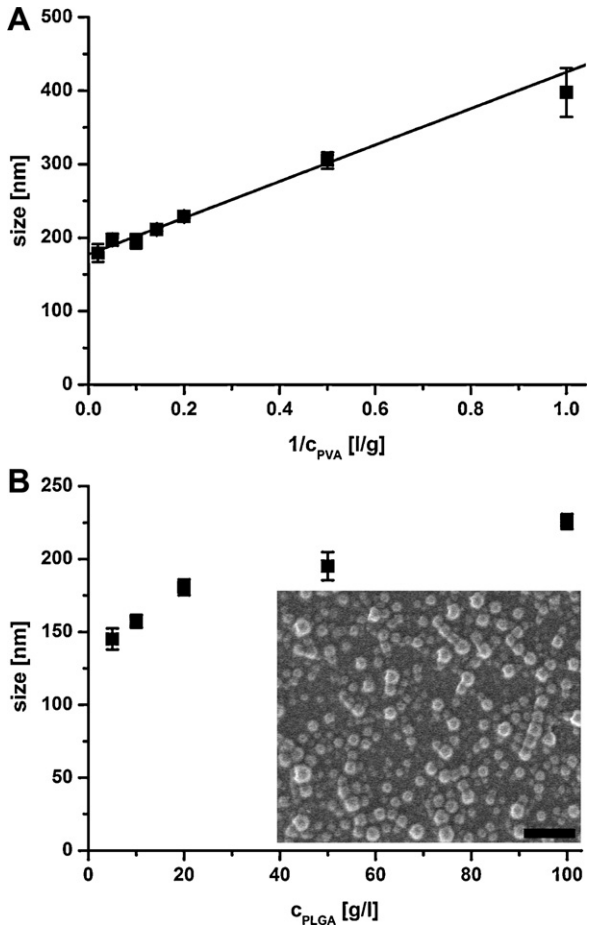

Fig. 1. Influence of the inverse of the poly(vinyl alcohol) concentration ($1/c_{PVA}$) in the aqueous phase (A) and the poly(D,L-lactide-*co*-glycolide) concentration (c_{PLGA}) in the organic phase (B) on the particle size of nanoparticles prepared by the solvent evaporation technique. The straight line in (A) represents the linear fit of the experimental data ($R^2 = 0.991$). The inset in (B) shows a typical picture of nanoparticles from scanning electron microscopy (Scale bar = 1 μm). Values are presented as the mean ± S.D ($n = 4$).

suspension. Polydispersity index (PDI) decreased with higher stabilizer concentrations; PVA concentrations above 5 g/l resulted in PDI values below 0.1.

The sizes of nanoparticles as a function of PLGA concentration (c_{PLGA}) are displayed in Fig. 1B. The concentration of PVA was kept constant at 10 g/l, whereas PLGA concentration varied between 5 and 100 g/l. As the polymer concentration increased, the mean particle size of obtained nanoparticles changed from ~150 nm for a polymer concentration of 5 g/l to ~230 nm for a polymer concentration of 100 g/l. The PDI was found to be optimal (<0.1) between 10 and 50 g/l (data not shown).

Freshly prepared nanoparticles ($c_{PLGA} = 50$ g/l, $c_{PVA} = 10$ g/l) had a mean particle size of 195.1 ± 9.6 nm (mean ± S.D., $n = 4$) and a narrow PDI of 0.078 ± 0.002 (mean ± S.D., $n = 4$). The surface charge, displayed by the ζ-potential, was found to be negative (−5.7 ± 0.8 mV; mean ± S.D., $n = 4$). Nanoparticles were visualized by scanning electron microscopy and showed spherical shape (Fig. 1B, inset). Data from dynamic light scattering were in good agreement with results from SEM.

3.2. Factors affecting the aerosol performance of nanoparticle suspensions

All formulations were nebulized with the actively vibrating-mesh nebulizer Aeroneb® Pro. In order to compare the particle size distribution of the aerosolized formulations, the mass median aerodynamic diameter, the geometric standard deviation and the fine particle fraction of the aerosol was determined using laser diffraction. The output rate was determined gravimetrically. As described above, the nanoparticles were prepared by a solvent evaporation technique using PVA as stabilizer. Therefore, the impact of PVA on the nebulization process was evaluated first of all. PVA solutions with concentrations ranging from 1 to 15 g/l were investigated. Higher PVA concentrations were not nebulizable using the Aeroneb® Pro. The MMAD is illustrated as a function of PVA concentrations in Fig. 2A. As the PVA concentration was increased from 1 to 10 g/l, a decrease in MMAD from 5.1 ± 0.3 μm (mean ± S.D., $n = 4$) to 4.1 ± 0.2 μm (mean ± S.D., $n = 4$) was observed. A further increase of PVA concentration to 15 g/l led to larger aerosol droplets (MMAD = 4.5 ± 0.1 μm; mean ± S.D., $n = 4$). The GSD as a function of PVA concentrations is shown in Fig. 2B. A decrease of GSD of the aerosol droplets was observed over the whole PVA concentration range studied. While the GSD at a PVA concentration of 1 g/l was measured to be 1.89 ± 0.02 (mean ± S.D., $n = 4$), at a PVA concentration of 15 g/l the GSD was reduced to 1.66 ± 0.07 (mean ± S.D., $n = 4$). The FPF as a function of PVA concentrations is displayed in Fig. 2C. The FPF increased from 52.3 ± 3.8% (mean ± S.D., $n = 4$) to 67.1 ± 1.1% (mean ± S.D., $n = 4$) when the amounts of PVA present were increased from 1 to 10 g/l. A higher PVA concentration of 15 g/l led to a reduced FPF (62.9 ± 1.1%; mean ± S.D., $n = 4$). The output rate as a function of PVA concentrations is illustrated in Fig. 2D. The output rate decreased notable from 0.49 ± 0.03 g/min (mean ± S.D., $n = 4$) to 0.11 ± 0.02 g/min (mean ± S.D., $n = 4$) for PVA concentrations of 1 g/l and 15 g/l, respectively.

The nebulization performance of nanoparticle formulations as a function of nanoparticle concentration (2, 5 and 10 mg/ml) as well as PVA concentration (5, 7 and 10 g/l) is displayed in Fig. 3. The MMAD of the employed formulations gradually decreased as the PVA concentration was raised (Fig. 3A). The MMAD for nanoparticles prepared in 5 g/l PVA ranged between 4.7 ± 0.2 μm and 5.0 ± 0.2 μm (mean ± S.D., $n = 4$), while MMADs for nanoparticles prepared in 10 g/l PVA were found between 4.3 ± 0.1 μm and 4.4 ± 0.1 μm (mean ± S.D., $n = 4$). The GSD of the employed formulations successively dropped as the PVA concentration was increased (Fig. 3B). Nanoparticles prepared in 5 g/l PVA had GSDs between 1.82 ± 0.03 and 1.86 ± 0.03 (mean ± S.D., $n = 4$). The GSD for nanoparticles prepared in 10 g/l PVA was between 1.71 ± 0.01 and 1.73 ± 0.04 (mean ± S.D., $n = 4$). The FPF of the employed formulations increases as the PVA concentration was raised (Fig. 3C). The FPF for nanoparticles prepared in 5 g/l PVA ranged from 53.6 ± 2.1% to 57.1 ± 2.9% (mean ± S.D., $n = 4$), while the FPF for nanoparticles prepared in 10 g/l PVA was between 62.6 ± 1.2% and 65.1 ± 0.8% (mean ± S.D., $n = 4$). The output rate of the employed formulations decreased as the PVA concentration was increased (Fig. 3D). The output rate for nanoparticles prepared in 5 g/l PVA was measured to be between 0.33 ± 0.04 g/min and 0.31 ± 0.02 g/min (mean ± S.D., $n = 4$). The output rate for nanoparticles prepared in 10 g/l PVA ranged from 0.17 ± 0.02 g/min to 0.18 ± 0.03 g/min (mean ± S.D., $n = 4$). Employed nanoparticle concentrations revealed to have no clear trend on the nebulization performance for a given PVA concentration.

The physicochemical properties of the employed formulations for nebulization are shown in Fig. 4. A linear escalation in the dynamic viscosity for PVA solutions was measured as the concentration was increased (Fig. 4A). The obtained value for 1 g/l was 0.941 ± 0.009 mPa s (mean ± S.D., $n = 4$) and 1.544 ± 0.033 mPa s (mean ± S.D., $n = 4$) for a PVA concentration of 15 g/l. The surface tension as a function of the PVA concentration showed no concentration dependency over the investigated concentration range (Fig. 4A). All studied PVA concentrations reduced the surface

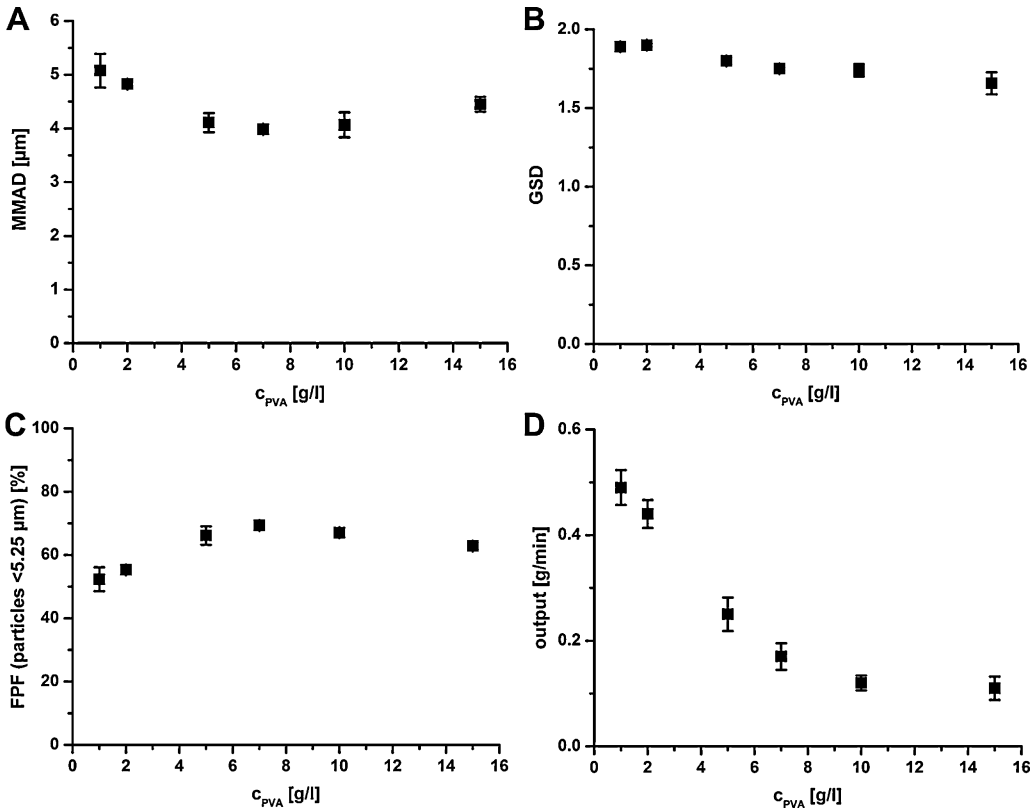

Fig. 2. Aerodynamic and output characteristics of poly(vinyl alcohol) solutions of different concentrations (c_{PVA}) nebulized with the Aeroneb® Pro. Aerodynamic properties were measured by laser diffraction, while the output rate was determined gravimetrically. Values are presented as the mean ± S.D ($n = 4$).

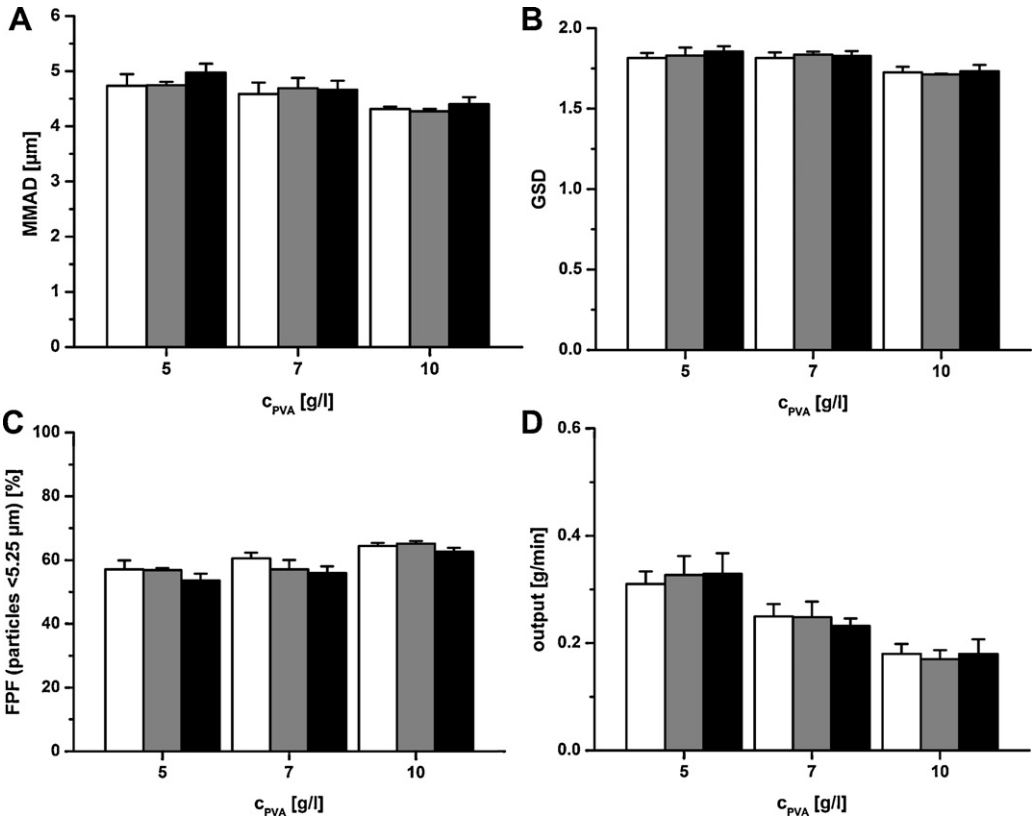

Fig. 3. Aerodynamic and output characteristics of different amounts of poly(D,L-lactide-*co*-glycolide) nanoparticles (open bars = 2 mg/ml, grey bars = 5 mg/ml and closed bars = 10 mg/ml) prepared in poly(vinyl alcohol) solutions of different concentrations (c_{PVA}) nebulized with the Aeroneb® Pro. Aerodynamic properties were measured by laser diffraction, while the output rate was determined gravimetrically. Values are presented as the mean ± S.D ($n = 4$).

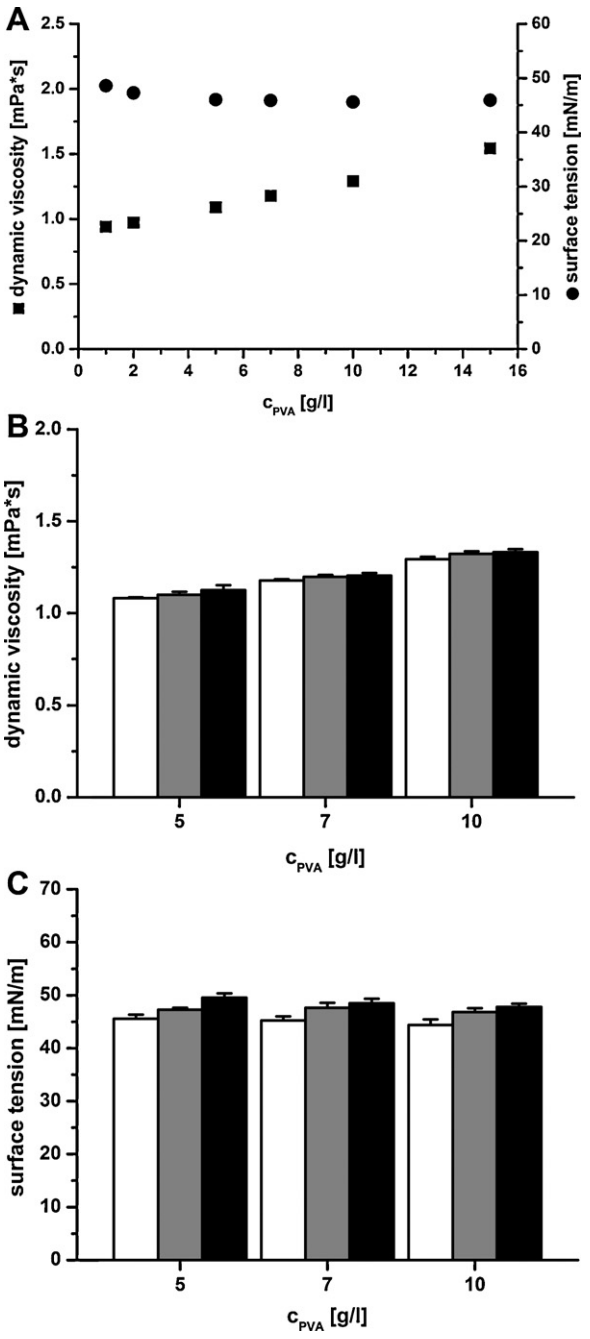

Fig. 4. Dynamic viscosities and surface tensions for poly(vinyl alcohol) solutions of different concentrations (c_{PVA}) (A) and for poly(D,L-lactide-*co*-glycolide) nanoparticles (open bars = 2 mg/ml, grey bars = 5 mg/ml and closed bars = 10 mg/ml) prepared in PVA solutions of different concentrations (B and C). Values are presented as the mean ± S.D ($n = 4$).

tension to values between 40 and 50 mN/m. The dynamic viscosity for different nanoparticle concentrations in PVA solutions of different concentration are displayed in Fig. 4B. Increasing the employed nanoparticle concentration for a given PVA concentration caused only a marginal change of dynamic viscosity of the employed formulations, while an escalation of the employed PVA concentration for a given nanoparticle concentration led to a considerably increased dynamic viscosity. At a PVA concentration of 5 g/l, dynamic viscosities of 1.081 ± 0.005 mPa s, 1.100 ± 0.016 mPa s and 1.125 ± 0.026 mPa s (mean ± S.D., $n = 4$) for a nanoparticle concentration of 2, 5 and 10 mg/ml were measured, respectively. A PVA concentration of 10 g/l caused dynamic viscosities of 1.294 ± 0.012 mPa s, 1.323 ± 0.015 mPa s and 1.332 ± 0.0163 mPa s (mean ± S.D., $n = 4$) for a nanoparticle concentration of 2, 5 and 10 mg/ml, respectively. The alteration of surface tension for different nanoparticle concentrations in PVA solutions of different concentration is shown in Fig. 4C. Keeping the PVA concentration constant at 5, 7 and 10 g/l and increasing the employed nanoparticle concentration led to considerably increased surface tension of the employed formulations, but keeping the nanoparticle concentration constant at 2, 5 and 10 mg/ml and escalating the employed PVA concentration caused only a marginal change of surface tension of the employed formulation. While surface tensions of 45.6 ± 0.8 mN/m, 45.3 ± 0.8 mN/m and 44.4 ± 1.1 mN/m (mean ± S.D., $n = 4$) were measured at a nanoparticle concentration of 2 mg/ml and PVA concentrations of 5, 7 and 10 g/l, surface tensions of 49.5 ± 0.8 mN/m, 48.5 ± 0.9 mN/m and 47.8 ± 0.6 mN/m (mean ± S.D., $n = 4$) at a nanoparticle concentration of 10 mg/ml and PVA concentrations of 5, 7 and 10 g/l were obtained.

3.3. Factors affecting the nanoparticle stability during nebulization

The stability of nanoparticles prepared in PVA solutions of different concentrations to nebulization with the vibrating-mesh nebulizer Aeroneb® Pro is shown as final to initial particle size (s_f/s_i) and polydispersity index (PDI_f/PDI_i) ratio for different amounts of nanoparticles (Fig. 5). The nebulized nanoparticle suspension was collected and investigated using DLS and SEM. Only negligible changes of particle size after nebulization were seen for all investigated PVA and nanoparticle concentrations (Fig. 5A). The PDI_f/PDI_i ratio only disclosed signs of instability to nebulization for high nanoparticle concentrations prepared in low amounts of PVA (nanoparticle concentrations of 5 and 10 mg/ml, PVA concentration of 5 g/l) (Fig. 5B). Moreover, the particle morphology, particle size and particle size distribution as seen by SEM for nebulized nanoparticles remained unchanged (Fig. 5C).

The thickness of the adsorbed PVA layer on nanoparticles was determined by three different techniques. The first one involved the preparation of uncoated nanoparticles by a nanoprecipitation technique (Beck-Broichsitter et al., 2010b). The prepared nanoparticles composed of PLGA had a mean size of 171.7 ± 3.5 nm (mean ± S.D., $n = 4$). This particle size is comparable to that of PLGA nanoparticles prepared by the solvent evaporation technique in this study. The uncoated nanoparticles were then incubated in PVA solutions of varying concentrations (0.001–10 g/l) and the increase in nanoparticle size due to adsorption of PVA on nanoparticles was determined by DLS. The obtained coating layer thickness for PVA on uncoated nanoparticles as a function of PVA concentration is found in the plateau of the adsorption isotherm in Fig. 6A and amounted to ~15 nm. The second method to determine the thickness of the adsorbed PVA layer on nanoparticles involved the measurement of the ζ-potential of nanoparticles prepared by the solvent evaporation technique as a function of electrolyte concentration. Freshly prepared and nebulized nanoparticles were incubated with different amounts of NaCl (0–5 mM) and the ζ-potential was measured. As the electrolyte concentration was heightened, an exponential change in ζ-potential was determined. Nanoparticles in distilled water (0 mM NaCl) had a ζ-potential of ~−40 mV, while a NaCl concentration of 5 mM resulted in a ζ-potential of ~−2 mV (Fig. 6B). No difference was seen between freshly prepared and nebulized nanoparticles. Plotting of $\ln(|\zeta\text{-potential}|)$, versus $3.33c^{1/2}$ for freshly prepared and nebulized nanoparticles yielded straight lines. The thickness of the adsorbed polymer layer is given by the slope (κ) of the corresponding lines of regression. In this manner the plot for freshly prepared and nebulized nanoparticles gave adsorbed PVA layer thicknesses of 13.4 ± 0.4 nm (mean ± S.D., $n = 4$; $R^2 = 0.995$) and 13.8 ± 0.9 nm (mean ± S.D., $n = 4$; $R^2 = 0.999$), respectively. No

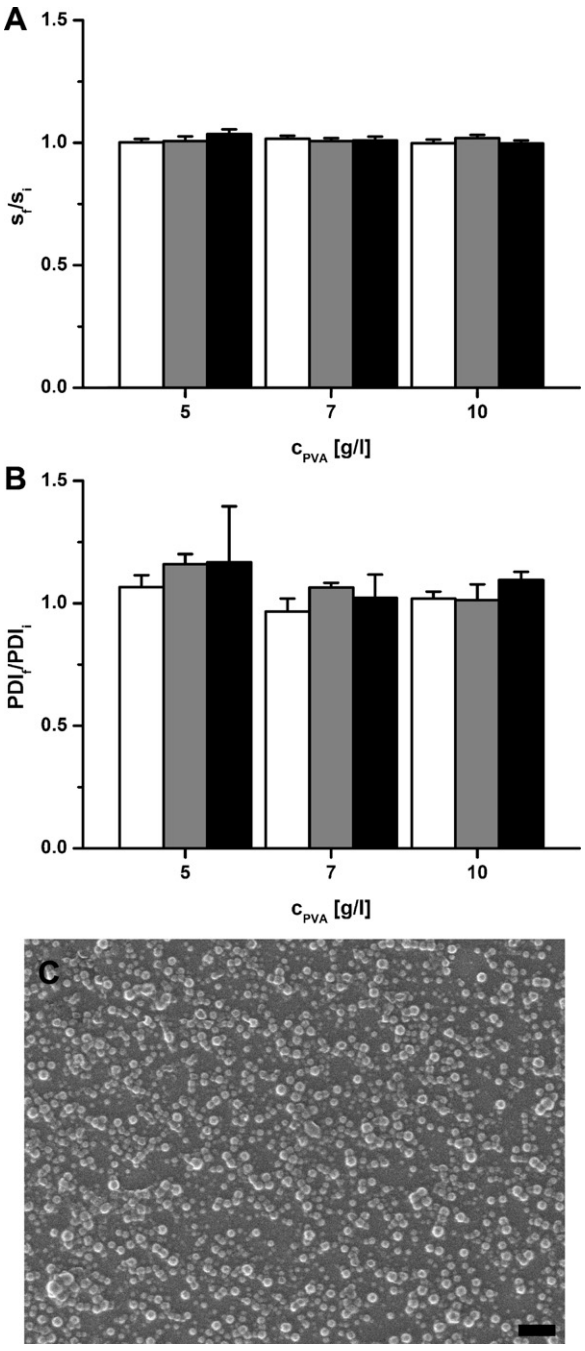

Fig. 5. Stability of poly(D,L-lactide-*co*-glycolide) nanoparticles prepared in poly(vinyl alcohol) solutions of different concentrations (c_{PVA}) to nebulization with the Aeroneb® Pro. The stability is shown as final to initial particle size (s_f/s_i) (A) and polydispersity index (PDI_f/PDI_i) (B) ratio for different amounts of nanoparticles (open bars = 2 mg/ml, grey bars = 5 mg/ml and closed bars = 10 mg/ml). A representative scanning electron microscopy picture of nebulized nanoparticles is shown in (C) (Scale bar = 1 μm). Aliquots of nanoparticle suspensions were collected during nebulization for analysis of nanoparticle stability to nebulization. Values are presented as the mean ± S.D ($n = 4$).

statistically significant difference between the thicknesses of the adsorbed PVA layer of freshly prepared and nebulized particles was found. The third applied method for the determination of the thickness of the adsorbed PVA layer on nanoparticles prepared by the solvent evaporation technique involved the use of transmission electron microscopy (TEM). The adsorbed polymer layer is visible in TEM as a thin corona around the nanoparticle (Fig. 6D). The determined PVA thickness on nanoparticles from TEM ranged between 10 and 20 nm. Overall, the results from the three employed methods for the determination of the adsorbed PVA layer thickness were in good agreement.

3.4. Stability of sildenafil-loaded nanoparticles to nebulization

Sildenafil-loaded PLGA nanoparticles were prepared with a theoretical drug loading of 5% (w/w). For that purpose, 2 ml of the organic phase containing polymer and drug (in total 50 mg/ml) were transferred to 10 ml of an aqueous phase containing 10 g/l PVA as stabilizer. The aqueous phase was adjusted to pH 8 with 4-(2-Hydroxyethyl)piperazine-1-ethanesulfonic acid-sodium salt. Freshly prepared sildenafil-loaded nanoparticles were of spherical shape, showed a mean particle size of 197.1 ± 1.7 nm (mean ± S.D., $n = 4$) and a narrow particle size distribution (PDI = 0.074 ± 0.005, mean ± S.D., $n = 4$). The surface charge, displayed by the ζ-potential, was found to be negative (−5.1 ± 0.3 mV; mean ± S.D., $n = 4$). The actual sildenafil content was 4.05 ± 0.15% (w/w) (mean ± S.D., $n = 4$), corresponding to an encapsulation efficiency of ∼80%.

The aerodynamic and output characteristics of NaCl 0.9% (*m*/*v*) and sildenafil-loaded nanoparticles when nebulized with the Aeroneb® Pro together with the physicochemical properties of the two formulations are given in Table 1. The prepared nanoparticle formulations had a significantly smaller MMAD, GSD and output rate compared to NaCl 0.9% (*m*/*v*) ($p < 0.05$). The FPF for sildenafil-loaded nanoparticles was significantly increased ($p < 0.05$). The nanosuspensions exhibited a significantly higher dynamic viscosity and lower surface tension compared to NaCl 0.9% (*m*/*v*) ($p < 0.05$).

The stability of sildenafil-loaded nanoparticles to nebulization is shown as final to initial nanoparticle property ($property_f/property_i$) ratio (Fig. 7). Aliquots of nanoparticle suspensions were collected during nebulization and the stability of the nebulized nanoparticle suspensions was investigated using DLS and SEM. In addition, the amount of encapsulated sildenafil of the aerosolized sildenafil-loaded nanoparticles was estimated. Nebulized sildenafil-loaded nanoparticles showed no signs of physical instability to nebulization. Particle size, PDI and drug content remained unchanged after nebulization (Fig. 7A). Moreover, no change of particle morphology, particle size and particle size distribution was seen in SEM (Fig. 7B).

The *in vitro* sildenafil release from the nanoparticle formulations before and after nebulization is displayed in Fig. 8. Free sildenafil powder served as a control. The free drug was immediately dissolved in the release medium (≤15 min). No loss of sildenafil was detected. Freshly prepared sildenafil-loaded nanoparticles released the whole encapsulated amount of sildenafil (>95%) during incubation time. A sustained release of sildenafil was observed over ∼120 min. The drug release behavior of sildenafil-loaded nanoparticles was not affected by nebulization and the release pattern of nebulized nanoparticles superimposed that of freshly prepared nanoparticles.

4. Discussion

4.1. Factors affecting the preparation of nanoparticles by the solvent evaporation technique

Several strategies have been proposed for the preparation of polymeric nanoparticles used as drug delivery systems in the field of nanomedicine. Among the numerous manufacturing procedures, the solvent evaporation technique is known to be a convenient method for the production of biodegradable nanoparticles (Vauthier and Bouchemal, 2009). The preparation of nanoparticles composed of poly(D,L-lactide-*co*-glycolide) by the solvent evaporation technique involved the emulsification of an organic PLGA solution in an aqueous phase containing poly(vinyl alcohol) as

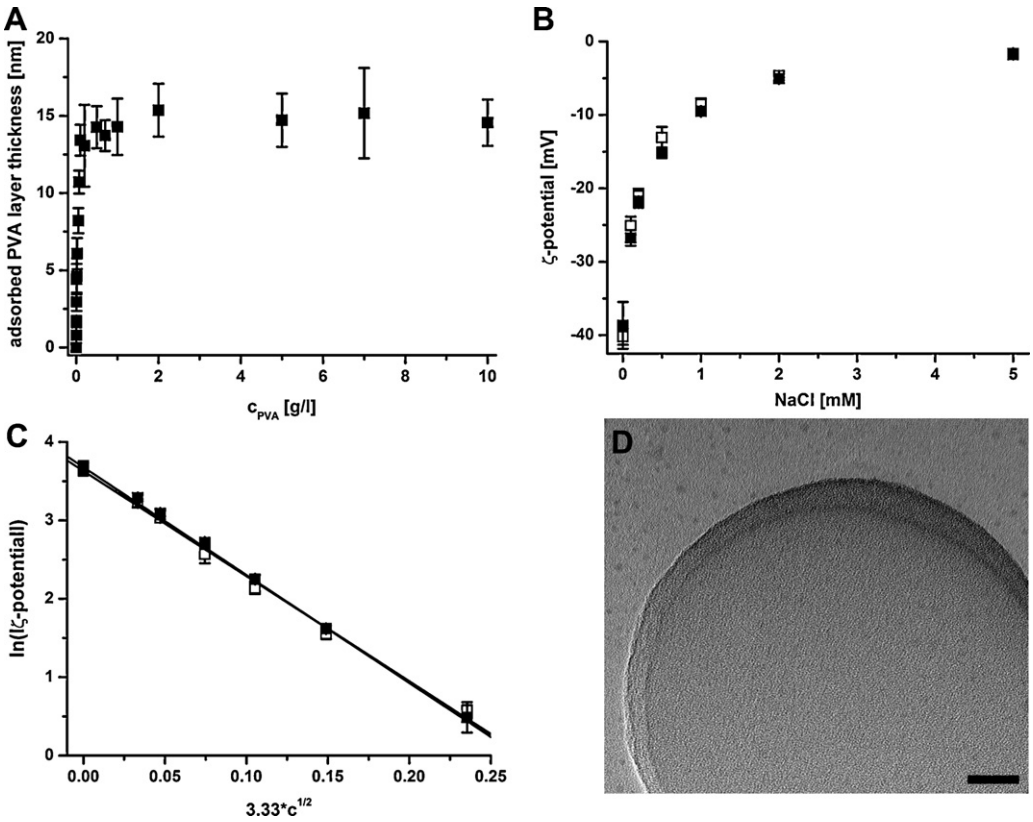

Fig. 6. Adsorbed poly(vinyl alcohol) layer thickness on poly(D,L-lactide-*co*-glycolide) nanoparticles as a function of PVA concentration (c_{PVA}) (A) and ζ-potential of PLGA nanoparticles prepared in PVA solutions shown as a function of electrolyte concentration (B). The slope (κ) of the ln|ζ-potential| versus $3.33c^{1/2}$ plot gives the thickness of the adsorbed polymer layer (C). Open and closed symbols in (B) and (C) represent characteristics of freshly prepared and nebulized nanoparticles, respectively. The straight lines in (C) represent linear fits of the experimental data ($R^2 > 0.99$). The adsorbed polymer layer is also visible in the representative transmission electron microscopy picture (D) (Scale bar = 20 nm). Values are presented as the mean ± S.D ($n = 4$).

surface active stabilizer. After emulsification the organic phase was removed by evaporation and the polymer precipitated in the form of colloidal particles. The size of obtained nanoparticles was on the one hand a function of the employed PVA concentration and on the other hand a function of the applied PLGA concentration (Fig. 1). Small nanoparticles (~200 nm) with narrow size distributions were obtained at increasing PVA concentrations, as it is already described for various surface active agent/polymer combinations (Bazile et al., 1992; Beck-Broichsitter et al., 2011b; Bodmeier and Chen, 1990; Desgouilles et al., 2003; Lamprecht et al., 1999; Scholes et al., 1993). Thus, the limiting factor to get smaller nanoparticles is the ability of the surface active agent to occupy the new interface formed between organic and aqueous phase. The sufficient coverage of the emulsion droplet surface with the stabilizer (PVA) evoked an improved stability of the emulsion droplets from coalescence and consequently led to smaller nanoparticles after solvent evaporation (Fig. 1A). The reduction of nanoparticle size upon lowering of the polymer amount in the organic phase is attributed to a lower viscosity of the dispersed phase (Fig. 1B) (Lamprecht et al., 1999; Scholes et al., 1993). In this study, optimal nanoparticle preparation conditions were found for a PVA concentration of 10 g/l combined with a PLGA concentration of 50 g/l.

4.2. Factors affecting the aerosol performance of nanoparticle suspensions

Over the past decades the generation of therapeutic aerosols has primarily been reserved to pneumatic- and ultrasound-driven nebulizers. Recent technological advances have led to improved nebulizer design employing vibrating-mesh technology for aerosol generation, like for example implemented in the Aeroneb® Pro device (Dhand, 2002; Waldrep and Dhand, 2008). Vibrating-mesh nebulizers have been shown to overcome the main drawbacks of pneumatic- and ultrasound-driven nebulizers, i.e. concentration of medicaments and temperature changes inside the nebulizer reservoir, high residual volumes and induction of nanoparticle aggregation during nebulization (Dailey et al., 2003a,b; Dhand, 2002; Waldrep and Dhand, 2008). The aerodynamic characteristics of aerosols generated by the Aeroneb® Pro were shown to be significantly affected by the physicochemical properties, like surface tension, viscosity and ion concentration of the fluids applied

Table 1
Aerodynamic, output and physicochemical characteristics of the employed formulations.

Formulation	MMAD[a] [μm]	GSD[b]	FPF[c] [%]	Output [g/min]	Dynamic viscosity [mPa s]	Surface tension [mN/m]
NaCl 0.9% (*m*/*v*)	4.9 ± 0.1	1.94 ± 0.02	54.9 ± 1.9	0.53 ± 0.04	0.923 ± 0.004	70.3 ± 0.5
Sildenafil-loaded nanoparticles	4.6 ± 0.1*	1.77 ± 0.04*	60.5 ± 2.4*	0.19 ± 0.05*	1.332 ± 0.016*	47.8 ± 0.6*

Values are presented as the mean ± S.D. ($n = 4$). The asterisks denote statistically significant differences compared to NaCl 0.9% (*m*/*v*) ($p < 0.05$).

[a] Mass median aerodynamic diameter.
[b] Geometric standard deviation.
[c] Fine particle fraction.

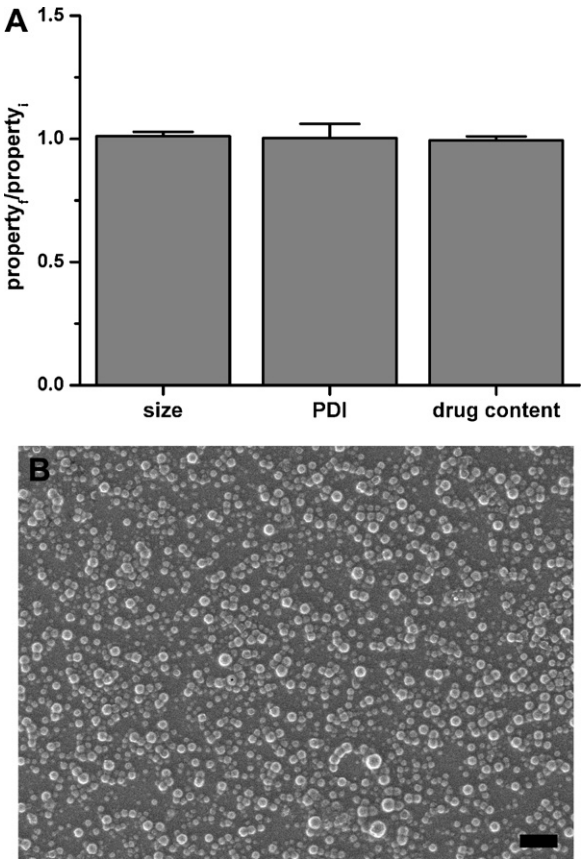

Fig. 7. Stability of sildenafil-loaded poly(D,L-lactide-co-glycolide) nanoparticles to nebulization with the Aeroneb® Pro. The stability is shown as final to initial nanoparticle property (property$_f$/property$_i$) ratio (A) (PDI = polydispersity index). A representative scanning electron microscopy picture of nebulized nanoparticles is shown in (B) (Scale bar = 1 μm). Aliquots of nanoparticle suspension were collected during nebulization for analysis of nanoparticle stability to nebulization. Values are presented as the mean ± S.D (n = 4).

for nebulization. For example, an increased viscosity resulted in smaller aerosol droplets and increased fine particle fraction. Beside the aerodynamic characteristics, other important attributes are also influenced by the physicochemical properties of the used fluids, like

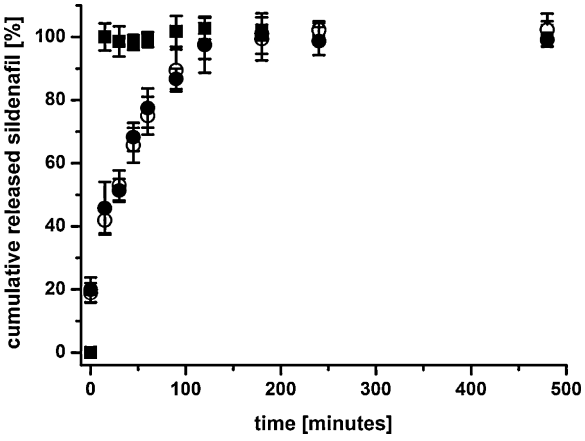

Fig. 8. *In vitro* drug release profiles of sildenafil-loaded poly(D,L-lactide-*co*-glycolide) nanoparticles (circles). Open symbols represent release characteristics of freshly prepared sildenafil-loaded nanoparticles, whereas closed symbols show the release characteristics of nebulized sildenafil-loaded nanoparticles. Aliquots of nanoparticle suspension were collected during nebulization for analysis of the impact of nebulization on the release profile of sildenafil from nanoparticles. For comparison the dissolution profile of sildenafil powder (closed squares) in the release medium is also included. Values are presented as the mean ± S.D (n = 4).

output rate. In general, an increased viscosity led to a prolonged nebulization time and reduced output rate (Ghazanfari et al., 2007; Zhang et al., 2007). Similar effects were observed in this study, when we measured the aerodynamic and output characteristics for PVA solutions and for nanoparticle-containing PVA solutions. An increase in PVA concentration decreased the mass median aerodynamic diameter, the geometric standard deviation and increased the FPF. A higher viscosity led to a prolonged nebulization time and reduced output rate (Figs. 2 and 4A). The surface tension of nebulized fluids had minor influence on the nebulization properties in this study (Fig. 4A).

The presence of nanoparticles disclosed trends comparable to that of PVA solution alone. A gradual decrease of MMAD and GSD was observed, while the FPF was gradually increased. A potent decay in output rate was detected as the PVA concentration was escalated. The investigated nanoparticle concentration ranges revealed no clear trend on the nebulization performance for a given PVA concentration (Fig. 3). This behavior is attributed to the viscosity characteristics as a function of PVA concentration (Fig. 4B). The presence of nanoparticles was shown to have an influence on the surface tension of PVA solutions, but was of minor importance on the nebulization characteristics of the used formulations (Fig. 4C). Higher nanoparticle concentrations (higher total surface area) "immobilized" more PVA on their surface and impeded the PVA to reduce the surface tension at the air–water interface.

4.3. Factors affecting the nanoparticle stability during nebulization

The nanoparticle production process necessitated the addition of a surface active agent (PVA) to the continuous aqueous phase. During emulsification, PVA binds tightly to the newly created interface which leads to coverage of the nanoparticle surface after the solvent has been removed. Hence, a thin protective layer is formed around the nanoparticles during preparation.

The aggregation of nanoparticles during aerosolization is dependent on both the nanoparticle surface characteristics and the technique for aerosol generation. Dailey et al. (2003a) showed a reduced aggregation tendency for nanoparticles exhibiting a more hydrophilic surface. Coating of nanoparticle surfaces with hydrophilic polymers was also shown to improve the nebulization stability of biodegradable nanoparticles (Dailey et al., 2003b). Furthermore, the use of vibrating-mesh nebulizers is suitable for the aerosolization of sensitive structures, like biodegradable nanoparticles (Dhand, 2002; Waldrep and Dhand, 2008). Indeed, biodegradable nanoparticles were not affected by nebulization using the Aeroneb® Pro as demonstrated by atomic force microscopy and dynamic light scattering (Beck-Broichsitter et al., 2009). A similar result was obtained in the current study, where size, size distribution and morphology of nanoparticles showed to be unaffected by forces generated during aerosolization (Fig. 5).

The thin protective PVA layer formed around the nanoparticles during the preparation is thought to improve the nebulization stability. Adsorbed polymers have been often found to modulate the physicochemical and biological properties of the employed nanoparticles (Besheer et al., 2009; Dailey et al., 2003b; Sahoo et al., 2002; Stolnik et al., 2001). Common techniques for the analysis of nanoparticle surfaces include X-ray photoelectron spectroscopy, Fourier transform infrared spectroscopy and static secondary ion mass spectrometry (Mu et al., 2004; Scholes et al., 1999). Polymer coated nanoparticles are furthermore characterized by means of DLS, laser Doppler anemometry and transmission electron microscopy with regard to the determination of the adsorbed polymer layer thickness on nanoparticles. In this manner, we determined the adsorbed PVA layer thickness on nanoparticles to be between 10 and 20 nm by different methods (Fig. 6). No significant

change of the adsorbed PVA layer thickness was measured upon nebulization what affirmed our hypothesis. The determined PVA layer thickness on nanoparticles in this study was in the range of previously reported magnitudes for other surface active agent/polymer combinations (Besheer et al., 2009; Stolnik et al., 2001).

4.4. Stability of sildenafil-loaded nanoparticles to nebulization

The usefulness of polymeric nanoparticles as controlled drug delivery systems to the lung is limited to a successful encapsulation of the employed drug substance, in addition to the consideration of nebulization performance and nebulization stability, and is often limited to lipophilic drugs (Lebhardt et al., 2010; Rytting et al., 2008). As shown previously, the encapsulation of hydrophilic drugs in nanoparticles is a difficult task and strongly depends on the interaction of the therapeutic agent and the polymer that is used as nanoparticle matrix material (Beck-Broichsitter et al., 2009, 2010a, 2011b; Rytting et al., 2010). Manipulation of the pH of the aqueous phase was found to improve the encapsulation efficiency of various drugs in polymeric nanoparticles prepared by nanoprecipitation as well as by the solvent evaporation technique (Beck-Broichsitter et al., 2011b; Govender et al., 1999; Song et al., 1997; Ueda and Kreuter, 1997). Sildenafil is an amphoteric drug with a pH-dependent solubility profile, with limited solubility at neutral pH values (Wang et al., 2008). Hence, sildenafil-loaded nanoparticles were prepared in an aqueous phase with an adjusted pH value of 8 using a buffer salt. The entrapment of sildenafil into nanoparticles prepared by the solvent evaporation technique was not found to change the physicochemical properties of the nanoparticles significantly for a theoretical drug loading of 5% (w/w). The high sildenafil content in nanoparticles (~4% (w/w)) that was achieved under the above mentioned experimental conditions is attributed on the one hand to the affinity of sildenafil to the PLGA nanoparticle matrix and on the other hand to the adjustment of the aqueous pH value, that decreased the solubility of the drug in the aqueous phase and hence, caused minor drug leakage into this phase during nanoparticle formation.

As stated above, the aerodynamic and output characteristics of nanoparticles were a function of the viscosity of the employed formulation. The aerodynamic and output characteristics of sildenafil-loaded nanoparticles were comparable to the nebulization performance of blank PLGA nanoparticles prepared under identical conditions, but differed significantly from NaCl 0.9% (*m*/*v*) as nebulization medium. The decreased MMAD, GSD and output rate as well as the increased FPF are attributed to the higher viscosity of the employed nanoparticle formulations (Table 1). In this regard, surface tension seems to play a subordinate role. The higher output rate for NaCl 0.9% (*m*/*v*) is beside its lower viscosity also influenced by the high ion concentrations present. A high ion concentration increases the output rate of diverse liquids employing the Aeroneb® Pro as nebulizer at the expense of the aerodynamic properties of the produced aerosols (Ghazanfari et al., 2007; Zhang et al., 2007).

The physicochemical parameters associated with the stability of drug-loaded colloidal carriers like liposomes and lipid nanoparticles to nebulization have been addressed by a number of authors (Elhissi et al., 2007; Hureaux et al., 2009; Kleemann et al., 2007; Liu et al., 2008), but however, only scant information is available regarding the integrity of drug-loaded biodegradable nanoparticles after nebulization (Beck-Broichsitter et al., 2009, 2010a). Sildenafil-loaded nanoparticles used in this study showed only negligible changes in shape, particle size, particle size distribution (polydispersity index) and drug content after nebulization using the Aeroneb® Pro (Fig. 7). Again, the thin protective PVA layer around the nanoparticles is thought to improve the nebulization stability of nanoparticles, due to an increased nanoparticle surface hydrophilicity (Dailey et al., 2003a,b).

The release pattern from drug delivery systems is a key concern in the development of successful controlled release formulations used in the field of medicine and pharmacy. *In vitro* drug release studies are conducted with the aim to afford a rapid evaluation tool for developmental and quality control purposes. The *in vitro* release pattern is not intended to have one-to-one correlation with *in vivo* results, but as soon as animal data are available the *in vitro* model becomes quite useful as a quality control. Although the release from biodegradable nanoparticles *in vitro* is normally fast (several minutes to hours), prolonged pharmacological effects could be observed *ex vivo* and *in vivo* when drug-loaded nanoparticles were compared to free drug (Beck-Broichsitter et al., 2009, 2010a; Rytting et al., 2010). These studies demonstrated excellent agreement of the *in vitro* results with the effects observed in biological systems, thereby serving as examples highlighting the importance of *in vitro* release studies. In the present study, free sildenafil was rapidly dissolved in the release medium (≤15 min), whereas a sustained drug release was observed over ~120 min for freshly prepared sildenafil-loaded nanoparticles (Fig. 8). The entrapment of sildenafil within the nanoparticle matrix implied a longer distance for sildenafil to diffuse out of the particles, resulting in a significantly retarded drug release. This release behavior can be considered as an important improvement regarding the aerosol therapy of pulmonary arterial hypertension. Moreover, no difference in the release profile of sildenafil from nebulized nanoparticles compared to freshly prepared nanoparticles was observed, as nanoparticles were stable to nebulization using the Aeroneb® Pro.

5. Conclusion

The current study examined the properties of nanoparticulate drug delivery vehicles intended for pulmonary drug administration. Biodegradable nanoparticles were successfully synthesized using a solvent evaporation technique. The applied stabilizer during nanoparticle production was shown to influence the aerodynamic and output characteristics of aerosols generated using an actively vibrating-mesh nebulizer (Aeroneb® Pro) by creating an impact on formulation viscosity properties. The formed thin protective stabilizer layer around the nanoparticles improved the stability of nanoparticles to nebulization. Sildenafil was encapsulated into nanoparticles with high entrapment efficiency and the sildenafil-loaded nanoparticle formulation was transferred to an aerosol applicable for deposition in the respiratory part of the lung. Size, size distribution and sildenafil content of nanoparticles were not affected by nebulization. The prolonged drug release achieved with this novel pulmonary drug delivery system for sildenafil will lead to a decrease of administration frequency of drug-loaded nanoparticles compared to free drug and would therefore improve patients' convenience and compliance. Overall, the obtained sildenafil-loaded nanoparticles are a promising tool for the therapy of pulmonary arterial hypertension. Further studies will be carried out to firm up this hypothesis.

Conflict of interest

The authors disclose that no conflicting interests are associated with the manuscript. All authors have made substantial contributions to the article. All authors have approved the final article.

Acknowledgements

The authors would like to thank Michael Hellwig and Andreas K. Schaper (Department of Geosciences and Materials Science Center, University of Marburg) for their support with SEM and TEM.

This study was supported by the German Research Foundation (DFG). We want to express our sincere thanks for this grant.

References

Azarmi, S., Roa, W.H., Loebenberg, R., 2008. Targeted delivery of nanoparticles for the treatment of lung diseases. Adv. Drug Deliv. Rev. 60, 863–875.

Bazile, D.V., Ropert, C., Huve, P., Verrecchia, T., Marland, M., Frydman, A., Veillard, M., Spenleuhauer, G., 1992. Body distribution of fully biodegradable [^{14}C]-poly(lactic acid) nanoparticles coated with albumin after parenteral administration to rats. Biomaterials 13, 1093–1102.

Beck-Broichsitter, M., Gauss, J., Packhaeuser, C.B., Lahnstein, K., Schmehl, T., Seeger, W., Kissel, T., Gessler, T., 2009. Pulmonary drug delivery with aerosolizable nanoparticles in an ex vivo lung model. Int. J. Pharm. 367, 169–178.

Beck-Broichsitter, M., Gauss, J., Gessler, T., Seeger, W., Kissel, T., Schmehl, T., 2010a. Pulmonary targeting with biodegradable salbutamol-loaded nanoparticles. J. Aerosol Med. 23, 47–57.

Beck-Broichsitter, M., Rytting, E., Lebhardt, T., Wang, X., Kissel, T., 2010b. Preparation of nanoparticles by solvent displacement for drug delivery: a shift in the ouzo region upon drug loading. Eur. J. Pharm. Sci. 41, 244–253.

Beck-Broichsitter, M., Schmehl, T., Seeger, W., Gessler, T., 2011a. Evaluating the controlled drug delivery properties of inhaled nanoparticles using isolated, perfused, and ventilated lung models. J. Nanomater. (Article ID 163791).

Beck-Broichsitter, M., Schmehl, T., Gessler, T., Seeger, W., Kissel, T., 2011b. Development of a biodegradable nanoparticle platform for sildenafil: formulation optimization by factorial design analysis combined with application of charge-modified branched polyesters. J. Control. Release, doi:10.1016/j.jconrel.2011.09.058.

Besheer, A., Vogel, J., Glanz, D., Kressler, J., Groth, T., Maeder, K., 2009. Characterization of PLGA nanospheres stabilized with amphiphilic polymers: hydrophobically modified hydroxyethyl starch vs pluronics. Mol. Pharm. 6, 407–415.

Bodmeier, R., Chen, H., 1990. Indomethacin polymeric nanosuspensions prepared by microfluidization. J. Control. Release 12, 223–233.

Clark, A.R., 1995. The use of laser diffraction for the evaluation of the aerosol clouds generated by medical nebulizers. Int. J. Pharm. 115, 69–78.

D'Alonzo, G.E., Barst, R.J., Ayres, S.M., Bergofsky, E.H., Brundage, B.H., Detre, K.M., Fishman, A.P., Goldring, R.M., Groves, B.M., Kernis, J.T., Levy, P.S., Pietra, G.G., Reid, L.M., Reeves, J.T., Rich, S., Vreim, C.E., Williams, G.W., Wu, M., 1991. Survival in patients with primary pulmonary hypertension. Results from a national prospective registry. Ann. Intern. Med. 115, 343–349.

Dailey, L.A., Schmehl, T., Gessler, T., Wittmar, M., Grimminger, F., Seeger, W., Kissel, T., 2003a. Nebulization of biodegradable nanoparticles: impact of nebulizer technology and nanoparticle characteristics on aerosol features. J. Control. Release 86, 131–144.

Dailey, L.A., Kleemann, E., Wittmar, M., Gessler, T., Schmehl, T., Roberts, C., Seeger, W., Kissel, T., 2003b. Surfactant-free, biodegradable nanoparticles for aerosol therapy based on the branched polyesters, DEAPA-PVAL-g-PLGA. Pharm. Res. 20, 2011–2020.

Desgouilles, S., Vauthier, C., Bazile, D., Vacus, J., Grossiord, J.L., Veillard, M., Couvreur, P., 2003. The design of nanoparticles obtained by solvent evaporation: a comprehensive study. Langmuir 19, 9504–9510.

Dhand, R., 2002. Nebulizers that use a vibrating mesh or plate with multiple apertures to generate aerosol. Respir. Care 47, 1406–1418.

Elhissi, A.M.A., Faizi, M., Naji, W.F., Gill, H.S., Taylor, K.M.G., 2007. Physical stability and aerosol properties of liposomes delivered using an air-jet nebulizer and a novel micropump device with large mesh apertures. Int. J. Pharm. 334, 62–70.

Galie, N., Ghofrani, H.A., Torbicki, A., Barst, R.J., Rubin, L.J., Badesch, D., Fleming, T., Parpia, T., Burgess, G., Branzi, A., Grimminger, F., Kurzyna, M., Simonneau, G., 2005. Sildenafil citrate therapy for pulmonary arterial hypertension. N. Engl. J. Med. 353, 2148–2157.

Galie, N., Hoeper, M.M., Humbert, M., Torbicki, A., Vachiery, J.L., Barbera, J.A., Beghetti, M., Corris, P., Gaine, S., Gibbs, J.S., Gomez-Sanchez, M.A., Jondeau, G., Klepetko, W., Opitz, C., Peacock, A., Rubin, L., Zellweger, M., Simonneau, G., Vahanian, A., Auricchio, A., Bax, J., Ceconi, C., Dean, V., Filippatos, G., Funck-Brentano, C., Hobbs, R., Kearney, P., McDonagh, T., McGregor, K., Popescu, B.A., Reiner, Z., Sechtem, U., Sirnes, P.A., Tendera, M., Vardas, P., Widimsky, P., Al Attar, N., Andreotti, F., Aschermann, M., Asteggiano, R., Benza, R., Berger, R., Bonnet, D., Delcroix, M., Howard, L., Kitsiou, A.N., Lang, I., Maggioni, A., Nielsen-Kudsk, J.E., Park, M., Perrone-Filardi, P., Price, S., Domenech, M.T.S., Vonk-Noordegraaf, A., Zamorano, J.L., 2009. Guidelines for the diagnosis and treatment of pulmonary hypertension. Eur. Heart J. 30, 2493–2537.

Gessler, T., Seeger, W., Schmehl, T., 2008. Inhaled prostanoids in the therapy of pulmonary hypertension. J. Aerosol Med. 21, 1–12.

Ghazanfari, T., Elhissi, A.M.A., Ding, Z., Taylor, K.M.G., 2007. The influence of fluid physicochemical properties on vibrating-mesh nebulization. Int. J. Pharm. 339, 103–111.

Ghofrani, H.A., Osterloh, I.H., Grimminger, F., 2006. Sildenafil: from angina to erectile dysfunction to pulmonary hypertension and beyond. Nat. Rev. Drug Discov. 5, 689–702.

Govender, T., Stolnik, S., Garnett, M.C., Illum, L., Davis, S.S., 1999. PLGA nanoparticles prepared by nanoprecipitation: drug loading and release studies of a water soluble drug. J. Control. Release 57, 171–185.

Hureaux, J., Lagarce, F., Gagnadoux, F., Vecellio, L., Clavreul, A., Roger, E., Kempf, M., Racineux, J.L., Diot, P., Benoit, J.P., Urban, T., 2009. Lipid nanocapsules: ready-to-use nanovectors for the aerosol delivery of paclitaxel. Eur. J. Pharm. Biopharm. 73, 239–246.

Ichinose, F., Erana-Garcia, J., Hromi, J., Raveh, Y., Jones, R., Krim, L., Clark, M.W.H., Winkler, J.D., Bloch, K.D., Zapol, W.M., 2001. Nebulized sildenafil is a selective pulmonary vasodilator in lambs with acute pulmonary hypertension. Crit. Care Med. 29, 1000–1005.

Kleemann, E., Schmehl, T., Gessler, T., Bakowsky, U., Kissel, T., Seeger, W., 2007. Iloprost-containing liposomes for aerosol application in pulmonary arterial hypertension: formulation aspects and stability. Pharm. Res. 24, 277–287.

Lamprecht, A., Ubrich, N., Hombreiro Perez, M., Lehr, C.M., Hoffman, M., Maincent, P., 1999. Biodegradable monodispersed nanoparticles prepared by pressure homogenization-emulsification. Int. J. Pharm. 184, 97–105.

Lebhardt, T., Roesler, S., Beck-Broichsitter, M., Kissel, T., 2010. Polymeric nanocarriers for drug delivery to the lung. J. Drug Deliv. Sci. Technol. 20, 171–180.

Liu, J., Gong, T., Fu, H., Wang, C., Wang, X., Chen, Q., Zhang, Q., He, Q., Zhang, Z., 2008. Solid lipid nanoparticles for pulmonary delivery of insulin. Int. J. Pharm. 356, 333–344.

Mu, L., Seow, P.H., Ang, S.N., Feng, S.S., 2004. Study on surfactant coating of polymeric nanoparticles for controlled delivery of anticancer drug. Colloid Polym. Sci. 283, 58–65.

Olschewski, H., Simonneau, G., Galie, N., Higenbottam, T., Naeije, R., Rubin, L.J., Nikkho, S., Speich, R., Hoeper, M.M., Behr, J., Winkler, J., Sitbon, O., Popov, W., Ghofrani, H.A., Manes, A., Kiely, D.G., Ewert, R., Meyer, A., Corris, P.A., Delcroix, M., Gomez-Sanchez, M., Siedentop, H., Seeger, W., 2002. Inhaled iloprost for severe pulmonary hypertension. N. Engl. J. Med. 347, 322–329.

Rytting, E., Nguyen, J., Wang, X., Kissel, T., 2008. Biodegradable polymeric nanocarriers for pulmonary drug delivery. Expert Opin. Drug Deliv. 5, 629–639.

Rytting, E., Bur, M., Cartier, R., Bouyssou, T., Wang, X., Krueger, M., Lehr, C.M., Kissel, T., 2010. In vitro and in vivo performance of biocompatible negatively-charged salbutamol-loaded nanoparticles. J. Control. Release 141, 101–107.

Sahoo, S.K., Panyam, J., Prabha, S., Labhasetwar, V., 2002. Residual polyvinyl alcohol associated with poly (D,L-lactide-co-glycolide) nanoparticles affects their physical properties and cellular uptake. J. Control. Release 82, 105–114.

Scholes, P.D., Coombes, A.G.A., Illum, L., Davis, S.S., Vert, M., Davies, M.C., 1993. The preparation of sub-200 nanometer poly(lactide-co-glycolide) microspheres for site-specific drug delivery. J. Control. Release 25, 145–153.

Scholes, P.D., Coombes, A.G.A., Illum, L., Davis, S.S., Watts, J.F., Ustariz, C., Vert, M., Davies, M.C., 1999. Detection and determination of surface levels of poloxamer and PVA surfactant on biodegradable nanospheres using SSIMS and XPS. J. Control. Release 59, 261–278.

Shimada, K., Miyagishima, A., Sadzuka, Y., Nozawa, Y., Mochizuki, Y., Ohshima, H., Hirota, S., 1995. Determination of the thickness of the fixed aqueous layer around polyethylene glycol-coated liposomes. J. Drug Target. 3, 283–289.

Song, C.X., Labhasetwar, V., Murphy, H., Qu, X., Humphrey, W.R., Shebuski, R.J., Levy, R.J., 1997. Formulation and characterization of biodegradable nanoparticles for intravascular local drug delivery. J. Control. Release 43, 197–212.

Stolnik, S., Daudali, B., Arien, A., Whetstone, J., Heald, C.R., Garnett, M.C., Davis, S.S., Illum, L., 2001. The effect of surface coverage and conformation of poly(ethylene oxide) (PEO) chains of poloxamer 407 on the biological fate of model colloidal drug carriers. Biochim. Biophys. Acta 1514, 261–279.

Ueda, M., Kreuter, J., 1997. Optimization of the preparation of loperamide-loaded poly(L-lactide) nanoparticles by high-pressure emulsification-solvent evaporation. J. Microencapsul. 14, 593–605.

Vauthier, C., Bouchemal, K., 2009. Methods for the preparation and manufacture of polymeric nanoparticles. Pharm. Res. 26, 1025–1058.

Waldrep, J.C., Dhand, R., 2008. Advanced nebulizer designs employing vibrating mesh/aperture plate technologies for aerosol generation. Curr. Drug Deliv. 5, 114–119.

Wang, Y., Chow, M.S.S., Zuo, Z., 2008. Mechanistic analysis of pH-dependent solubility and trans-membrane permeability of amphoteric compounds: application to sildenafil. Int. J. Pharm. 352, 217–224.

Wilkins, M.R., Wharton, J., Grimminger, F., Ghofrani, H.A., 2008. Phosphodiesterase inhibitors for the treatment of pulmonary hypertension. Eur. Respir. J. 32, 198–209.

Zhang, G., David, A., Wiedmann, T.S., 2007. Performance of the vibrating membrane aerosol generation device: aeroneb micropump nebulizer. J. Aerosol Med. 20, 408–416.